JRRD
Volume 41, Number 1, Pages 15–32
January/February 2004
Journal of Rehabilitation Research & Development

Effects of spinal cord injury on lower-limb passive joint moments revealed through a nonlinear viscoelastic model

Kofi Amankwah, MS; Ronald J. Triolo, PhD; Robert Kirsch, PhD
Biomedical Engineering Department, Case Western Reserve University, Cleveland, OH

Abstract—We developed a mathematical model to describe the lower-limb passive joint moments to investigate and compare these moments in a small sample of able-bodied volunteers and individuals with long-standing motor complete paraplegia. Isokinetic tests, which were performed on a sample of four subjects with spinal cord injuries (SCIs) and five uninjured individuals, measured the passive moments at the ankle, knee, and hip joints throughout their ranges of motion in the sagittal and coronal planes. We fitted an 11-parameter nonlinear viscoelastic model to the acquired passive moment data (mean square error ranging from 0.020 to 5.1 Nm^2) to compare subject populations and to determine the influences of joint velocity and passive coupling between adjacent joints. Although the passive moment curves of the SCI and able-bodied groups exhibited many similarities in shape, a repeated measures analysis of variance (ANOVA) that compared the passive moment curves of the two groups indicated a statistically significant ($p < 0.01$) difference for every joint except the knee. This new model for passive joint moments should prove to be useful in examining how changes in passive properties affect bipedal function and movement.

Key words: biological models, biomechanics, elasticity, nonlinear models, passive moments, spinal cord injury, viscoelasticity.

INTRODUCTION

The human musculoskeletal system includes structures, such as ligaments and joint capsules, that hold the joints together and help guide movements of bony surfaces relative to one another [1]. These structures contain collagen networks that generate resistive forces when stretched. Muscles produce active forces to generate movements, but they also contain collagenous structures, which hold the muscle fibers together and resist stretch even when the muscle is relaxed. Finally, the joints themselves exhibit resistance to movement because of the properties of cartilage and the shapes of the contacting articular surfaces [1]. Together, all of these resistive forces across a joint generate a *passive moment* about the joint.

Passive joint moments are among the elements of the musculoskeletal system involved in controlling movement. For example, a significant passive joint moment may increase the stability of the joint (e.g., locking of the knee at full extension). Unfortunately, inactivity of a joint often leads to chronic changes in the tissues surrounding it, ultimately altering the passive joint moments. Such inactivity

Abbreviations: ANOVA = analysis of variance, EMG = electromyographic, FES = functional electrical stimulation, MSE = mean square error, ROM = range of motion, SCI = spinal cord injury, SD = standard deviation, VA = Department of Veterans Affairs.

This material was based on work supported by funds from the Department of Veterans Affairs (VA) Predoctoral Fellowship, VA Center of Excellence in FES; National Institutes of Health (NIH)/National Center for Medical Rehabilitation Research (NCMRR) training grant HD-07500; NIH/ National Institutes of Neurological Disorders and Stroke (NINDS) N01-NS-6-2351; and NIH R01-NS-3-3756.

Address all correspondence to Ronald J. Triolo, PhD; Cleveland FES Center H601, 2500 MetroHealth Drive, Cleveland, OH 44119; 216-778-7877; fax: 216-778-4259; email: rxt24@po.cwru.edu.

can occur following spinal cord injury (SCI) if aggressive physical therapy is not maintained [2]. As a result, the lack of joint motion leads to shortening of ligaments, stiffening of joint capsules, and shortening of muscles [3–5]. In some cases, joint contractures develop and significantly limit range of motion (ROM) [2,6].

Early studies showed that the joint angle affects the passive moments [7–11], while others showed that the passive moments can also vary with the angular velocity of the joint [12–15]. More recently, the influence of biarticular muscles on the passive moment was illustrated [15–19]. Prior attempts to model passive joint moments mathematically described the nonlinear passive elastic properties as a combination of two exponential functions [15,17–24]. To characterize the viscous component of passive joint properties, researchers have used two approaches. One approach modeled the hysteresis arising from viscous effects by determining two separate sets of double exponential functions [13,25]: one for flexion to extension movements and one for extension to flexion movements. This approach however did not include the effects of stress-relaxation that occur in all connective tissues [1]. The second approach modeled the viscous joint properties as a power function of the joint velocity [13,26]. This approach provided a means to model stress-relaxation but only for one direction of movement at a time. Thus, existing information regarding human lower-limb passive joint properties was limited to the sagittal plane (i.e., flexion and extension of the ankle, knee, and hip), and current models of these properties have not been complete.

Passive joint moments also have an impact on the development of neuroprostheses that use functional electrical stimulation (FES) to restore standing and walking to individuals with paraplegia. In particular, the use of FES can be significantly hampered by changes in passive joint moments [27], especially when coupled with muscle weakness caused by disuse atrophy. Yet, many theoretical studies of lower-limb neuroprostheses neglect the changes in passive joint moments following SCI altogether [28].

The principal objective of this study was to quantify the effects of SCI on the lower-limb passive joint moments during both sagittal and nonsagittal motions, including the effects of joint rotational velocity and the positioning of adjacent joint angles. The specific goals of this study were (1) to measure the human lower-limb passive moments in both sagittal and coronal planes for able-bodied and SCI subjects, (2) to develop a single equation model that represents the salient features of the passive joint moments in a computationally efficient manner, and (3) to use the model to compare the passive joint moments between able-bodied individuals and individuals with paraplegia.

METHODS

Experimental Testing

Subjects

Experiments were performed on four individuals with paraplegia and five able-bodied individuals. The characteristics of each subject have been included in **Table 1**. The MetroHealth Medical Center and Cleveland Department of Veterans Affairs (VA) Medical Center Institutional Review Boards approved the experimental protocol, and each subject provided informed consent to participate.

Table 1.
Characteristics of subjects.

Subject	Age (yr)	Sex	Height (m)	Weight (kg)	Level of Spinal Lesion	Years Since Lesion
EL	41	M	1.73	86.2	T6	3
KO	29	F	1.68	56.7	C6	3
MR	36	M	1.75	90.7	T5	17
CZ	27	M	1.85	90.7	T8	2
CG	25	M	1.88	80.3	Able-Bodied	NA
TG	24	M	1.91	76.5	Able-Bodied	NA
LO	23	F	1.60	61.2	Able-Bodied	NA
MJ	29	F	1.57	47.5	Able-Bodied	NA
NO	25	M	1.77	72.9	Able-Bodied	NA

NA = not applicable

Procedures

Subjects were positioned in a Biodex System 3® dynamometer (www.Biodex.com) so that the rotational center of the joint of interest was aligned with the rotational center of the dynamometer spindle. The dynamometer rotated the primary joint at a constant velocity and measured the rotational velocity, the joint angle, and the passive moment developed at the joint. An example of the measured signals is shown in **Figure 1**. A force and moment transducer (JR3 Inc., www.JR3.com; model 160M50A-I100) was mounted to the spindle of the dynamometer to obtain higher resolution moment signals about all three axes. The moment data from the additional two off-plane axes were used to ensure that the center of rotation of the joint and the dynamometer were well aligned. In some cases, electronic goniometers (Biometrics Ltd., www.BiometricsLtd.com; model XM110) were also used to measure the primary or adjacent joint angles. The surfaces of the goniometers were affixed to the limbs with double-sided tape and then further secured with tape placed over the goniometers and limb.

The goniometers and joint position output of the dynamometer were referenced to the anatomical angles defined in **Figure 2**. The plantar flexion/dorsiflexion angle was defined as the angle between the surface of the foot, the lateral malleolus, and the lateral epicondyle of the femur. A plantar flexion angle of 0° was defined as the surface of the foot being perpendicular to the line

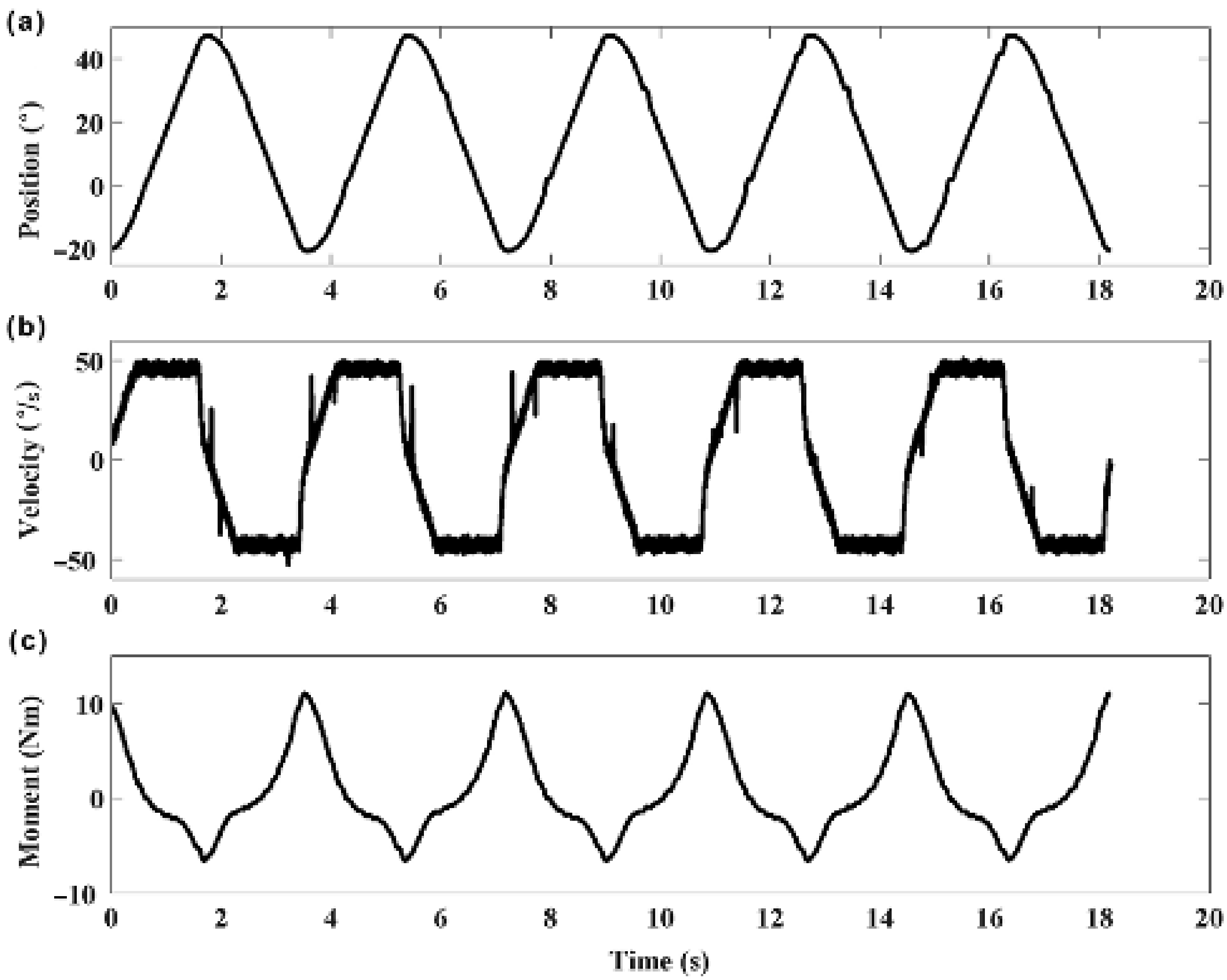

Figure 1.
Five cycles of data from one experimental trial. **(a)** Joint angle of ankle as it was rotated in plantar flexion/dorsiflexion direction. **(b)** Constant joint velocity magnitude of 45°/s applied to joint. **(c)** Measured passive joint moment at ankle.

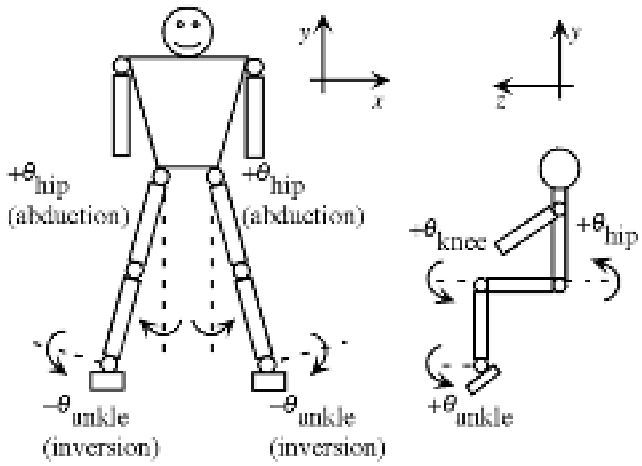

Figure 2.
Joint angle definitions.

through the lateral malleolus and lateral epicondyle of the femur. The ankle inversion/eversion angle was defined as the angle between the surface of the foot and the sagittal plane passing through the tibia. An ankle inversion angle of 0° was defined by the second metatarsal being in-line with the sagittal plane. The line passing through the lateral malleolus and lateral epicondyle of the femur and the line passing through the lateral epicondyle of the femur and the greater trochanter were used to define the knee joint angle. The knee angle was 0° when the knee was extended and the two lines were coincident. The hip flexion angle was determined by the line passing through the lateral epicondyle of the femur and greater trochanter and by the line through the greater trochanter and the anterior superior iliac crest. When the angle between these lines was 15°, the hip flexion angle was defined to be 0°. The hip abduction angle was defined by a line connecting the left and right anterior superior iliac crests and by a line connecting the patella and anterior superior iliac crest of the limb being measured. The abduction angle was 0° when these two lines were perpendicular. With these joint angle conventions, all joint angles would be near zero when the subject was standing erect.

Five separate experiments characterized the passive moments developed at the ankle, knee, and hip joints in the flexion/extension direction, the ankle joint in the inversion/eversion direction, and the hip joint in the abduction/adduction direction. For each joint measured, the same minimum range of motion (ROM) was used for each subject to ensure that sufficient passive moments developed at the ends of the ranges. If the subject's ROM was larger than the minimum ROM, the testing ROM was expanded until the subject just felt discomfort. For all the joints tested, the angular velocities and adjacent joint angles included those encountered during a sit-to-stand transition [29–32].

As in previous studies [23,27,33], the joint was preconditioned before the experiment began so that the passive moment measurements would not be history-dependent. The preconditioning consisted of cycling the joint through its ROM 20 times at an angular velocity of 10°/s. Following the preconditioning, we performed the seven isokinetic trials of the experiment. Each trial consisted of rotating the joint through 15 cycles of its ROM. The first 10 cycles continued the joint conditioning, while the last 5 cycles were used for the data analysis.

During the seven experimental trials, the angular joint velocity and the proximal and distal joint angles were varied. **Tables 2** to **6** illustrate, for each of the five joints measured, the values used during each trial for the angular joint velocities and adjacent joint angles. For the first three trials, external braces fixed the proximal and distal joints angles as we applied different constant angular velocities to examine the viscoelastic component of the passive joint moment [13,22,23,34]. During the next two trials, the primary joint was rotated through its ROM at a constant velocity as the proximal joint angle was fixed at one of two positions that were different from the initial proximal joint angle. Similarly for the last two trials, the distal joint angle was fixed at one of two new different positions. These last four trials examined the influence that biarticulate muscles crossing the proximal and primary joints or the distal and primary joints have on the passive moments of the primary joint.

Initially, to ensure that voluntary or involuntary muscle activity would not be a confounding factor, we monitored

Table 2.
Experimental conditions for ankle inversion/eversion.

Trial Number	Angular Velocity (°/s)	Proximal Joint Angle (°) (Ankle Flex/Ext)
1	5	0
2	10	0
3	30	0
4	10	–15
5	10	15

Note: Distal joint angle (°) does not apply.
Flex/Ext = flexion/extension.

Table 3.
Experimental conditions for ankle flexion/extension.

Trial Number	Angular Velocity (°/s)	Proximal Joint Angle (°) (Knee Flex/Ext)	Distal Joint Angle (°) (Ankle Inv/Ev)
1	5	0	0
2	10	0	0
3	30	0	0
4	10	40	0
5	10	80	0
6	10	0	–10
7	10	0	10

Flex/Ext = flexion/extension Inv/Ev = inversion/eversion

Table 4.
Experimental conditions for knee flexion/extension (flex/ext).

Trial Number	Angular Velocity (°/s)	Proximal Joint Angle (°) (Hip Flex/Ext)	Distal Joint Angle (°) (Ankle Flex/Ext)
1	5	0	0
2	60	0	0
3	90	0	0
4	10	20	0
5	10	80	0
6	10	0	10
7	10	0	–10

Table 5.
Experimental conditions for hip flexion/extension.

Trial Number	Angular Velocity (°/s)	Proximal Joint Angle (°) (Hip Ab/Ad)	Distal Joint Angle (°) (Knee Flex/Ext)
1	5	0	0
2	60	0	0
3	90	0	0
4	10	–5	0
5	10	15	0
6	10	0	40
7	10	0	80

Flex/Ext = flexion/extension Ab/Ad = abduction/adduction

the electromyographic (EMG) activities of relevant muscles (Cambridge Electronic Design Ltd., www.CED.co.uk; model CED® 1902). The relevant muscles for each tested joint include gastrocnemius and tibialis anterior for ankle plantar flexion/dorsiflexion, rectus femoris and biceps femoris for the knee joint, rectus femoris and gluteus maximus for hip flexion/extension, tibialis anterior and peroneus longus for ankle inversion/eversion, and adductor magnus and gluteus medius for hip abduction/adduction. During the experiments however, we found that any EMG activity caused a noticeable discontinuity in the moment measurements, which was consistent with observations reported in the literature [13,15,16,18,23]. Consequently, EMG recordings were not performed on every subject. Any cycle that

Table 6.
Experimental conditions for hip abduction/adduction.

Trial Number	Angular Velocity (°/s)	Distal Joint Angle (°) (Hip Flex/Ext)
1	5	0
2	60	0
3	90	0
4	10	–10
5	10	50

Note: Proximal joint angle (°) does not apply.
Flex/Ext = flexion/extension.

exhibited a discontinuity was assumed to contain muscle activity and was not included in the subsequent data analysis.

All transducer signals were collected with a 200 MHz Pentium® I computer using a National Instruments® data acquisition board (National Instruments Corp., www.NI.com; model AT-MIO-64E-3). A virtual instrument created in the software package Labview® (National Instruments Corp., www.NI.com; version 5.0.1) was developed so the data could be sampled at 100 Hz and saved to the hard disk of the computer. The EMG data were rectified and low-pass filtered (Butterworth filter, 20 Hz cutoff frequency) before they were recorded.

Data Analysis

Development of Nonlinear Viscoelastic Model

To capture the salient features of the passive joint moments from the experimental data, we developed a model based upon the Kelvin model for viscoelasticity (**Figure 3**) [1]. With this viscoelastic model, an elastic response, a stress-relaxation response, and a creep response could be characterized with a single equation. To represent the passive joint moments, the Kelvin model was adapted to include a nonlinear elastic element in parallel with both a linear elastic element and a nonlinear viscous element in series.

The moment, M_e, described the nonlinear passive elastic moment and was modeled with the traditional double exponential:

$$M_e = a_1 e^{(a_2\theta + a_3\theta_p + a_4\theta_d)\pi/180} + a_5 e^{(a_6\theta + a_7\theta_p + a_8\theta_d)\pi/180}, \quad (1)$$

where θ = primary joint angle (°), θ_p and θ_d = proximal and distal joint angles respectively (°), and a_i = estimated model parameter i = 1,2,3, . . . ,8.

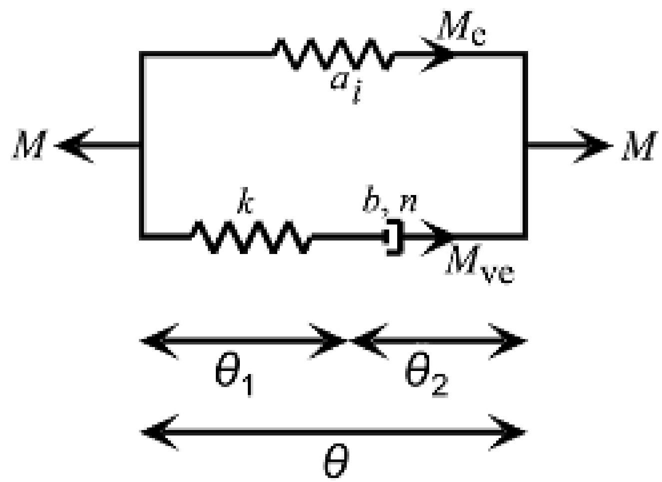

Figure 3.
Mechanical analogue of passive moment model. Two elastic (e) elements are represented with model parameters k and a_i, while parameters b and n characterize viscous (v) element. Joint angle is represented by θ, and M is passive moment developed at joint.

Parameter a_1 is a scaling factor for the exponential curve that represents joint extension, while parameter a_5 is a scaling factor that represents joint flexion. The parameters a_2 and a_6 indicate how the primary joint angle affects the passive joint moment. Parameters a_3 and a_7 and parameters a_4 and a_8 indicate the influence of the proximal and distal joint angles respectively on the passive joint moment and, therefore, reflect the influence of biarticulate muscles. Furthermore parameters a_2, a_3, and a_4 relate how these joint angles affect the moment as the joint is extended. Parameters a_6, a_7, and a_8 relate how these joint angles affect the joint moment in flexion.

The linear elastic element, M_{le}, which was in series with the viscous element, was modeled with the linear relationship

$$M_{le} = \angle k(\theta_1 \angle \theta_r) \ , \quad (2)$$

where θ_1 = joint angle across element (°), θ_r = neutral position for element (°), and k = estimated model parameter.

Because the model contains a viscous element, the addition of this series elastic element enables the model to perform a quick change in position without requiring an infinite moment to be applied. Parameter k represents the stiffness of the element; therefore, increases in k cause the element to become stiffer.

The viscous element, M_v, was modeled with a power function:

$$M_{\mathrm{v}} = -\mathrm{sgn}\left(\dot{\theta}_2\right)\left(b\left|\dot{\theta}_2\right|\right)^n \quad , \tag{3}$$

where

$$\mathrm{sgn}(x) = \begin{Bmatrix} +1 & x > 0 \\ \angle 1 & x < 0 \\ 0 & x = 0 \end{Bmatrix} \quad ,$$

$\dot{\theta}_2$ = velocity of element (°/s), and b and n = estimated model parameters. Equation (3) adds a velocity-dependent component to the model and captures the nonlinear relationship between the hysteresis and the joint angular velocity. Model parameter b represents the viscosity of the element. Since parameter n is an exponent with a value between 0 and 1, it represents how influential increases in velocity will be on the moment.

The following three equations represent relationships adapted from the Kelvin model:

$$M_{\mathrm{ve}} = M_{\mathrm{v}} = M_{\mathrm{le}} \quad ; \tag{4}$$

where M_{ve} = viscoelastic moment,

$$M = M_{\mathrm{e}} + M_{\mathrm{ve}} \quad ; \tag{5}$$

where M = total passive moment, and

$$\theta = \theta_1 + \theta_2 \quad . \tag{6}$$

To obtain a differential equation for the entire system, we first differentiated and substituted equation (2) into a differentiated equation (5). The resulting equation was

$$\dot{M} = \dot{M}_{\mathrm{e}} \angle k\dot{\theta}_1 \quad . \tag{7}$$

Equation (6) was then differentiated and substituted into equation (7) to yield

$$\dot{M} = \dot{M}_{\mathrm{e}} \angle k\dot{\theta} + k\dot{\theta}_2 \quad . \tag{8}$$

Substituting equation (3) into equation (8) for θ_2 and rearranging, the differential equation for the entire system became

$$\dot{M} = M_{\mathrm{e}} \angle k\dot{\theta} + \mathrm{sgn}\left(\dot{\theta}\right)\frac{k}{b}\left(\left|M_{\mathrm{e}} \angle M\right|\right)^{1/n} \quad . \tag{9}$$

Since the joint was rotated at a constant velocity, the solution to equation (9) was

$$M = M_{\mathrm{e}} \angle \mathrm{sgn}(\dot{\theta})(b|\dot{\theta}|)^n \angle \mathrm{sgn}(\dot{\theta})\left(\angle \frac{1}{\alpha\tau}(t \angle t_i) + \left|M_{\mathrm{ve}_i}\right|^{1/\alpha}\right)^{\alpha} \quad , \quad (10$$

where $\alpha = n/n - 1$, $\tau = b/k$, and M_{ve_i} = initial viscoelastic moment. Using equation (10), 11 model parameters must be estimated for each joint. The experimental protocol previously described was developed to ensure a sufficient set of data for the parameter estimation.

Analysis

The equation for the moment produced at a joint could be written as a combination of the passive and active moments plus the moment because of the weight of the limb:

$$M_{\mathrm{Measured}} = M_{\mathrm{Passive}} + M_{\mathrm{Active}} + M_{\mathrm{Limbweight}} \cos(\theta) \quad ,$$

where $M_{Measured}$ = measured moment (Nm) and θ = joint angle (°).

This equation does not include an inertial component, because the trials were performed at a constant angular velocity. Data points where the velocity was not constant because of the dynamometer changing its direction of rotation were not used in the analysis. Frictional moments were assumed to be negligible because of the low coefficient of friction (i.e., 0.002 – 0.020) at joints [1]. Since the muscles were assumed to be inactive (M_{Active} = 0), we determined the passive moment by subtracting $M_{Limbweight}$ from the measured moment. The moment caused by the limb weight consisted of two components. The first component was the moment caused by the weight of the Biodex attachments and any braces. We calculated this by measuring the moment developed when only the joint attachment and relevant brace were attached to the dynamometer. The second component, the moment caused by the weight of the limb itself, was calculated with the use of a regression equation developed by Zatsiorsky and Seluyanov [35]. Distance measurements from the center of gravity to the center of rotation of the limb were estimated as described by Zatsiorsky and Seluyanov and adapted according to de Leva [35,36]. The product of the estimated limb weight with the estimated distance to the center of rotation was used to approximate the moment caused by the weight of the limb. Although the regression equations yielded approximate values, they provided a consistent method for determining these values across all subjects and were necessary, since the experimental apparatus did not allow for joint positioning that eliminated the effects of gravity.

For each subject, the passive joint moments were measured under seven different conditions, and the last five cycles of data for each condition were ensemble-averaged. Using these averages, the model parameters of equation (6) were estimated with the nonlinear optimization routine *lsqcurvefit* (The Mathworks Inc., www.MathWorks.com; MatLab Release 12), which implements an algorithm based upon the interior-reflective Newton method to minimize the sum of the squared errors between the model output and the experimental data. The inputs to the optimization routine included the primary joint angle, primary joint velocity, positions of the proximal and distal joints, and the passive moments measured during each of the seven test conditions. The output of the routine was the 11 model parameters.

To obtain average properties for each subject group (able-bodied and SCI), we inputted the same standard set of joint angles and velocities into each subject's passive moment model to create a model data set. These data sets were then averaged across subjects, and model parameters were fitted to the averaged group data. The resulting model parameters were then used to represent the given subject group.

The model includes parameters for the proximal and distal joint angles; therefore, if these joints had no influence on the passive moments at a joint, the corresponding parameter values would be zero. The *F*-Test ($\alpha = 0.05$) was used to determine whether these parameters were significantly different from zero and therefore whether the adjacent joint angle influenced the passive moments [37]. Additionally, we determined the sensitivity of each parameter on the model output by examining the derivative of the model output with respect to each of the model parameters.

To examine and compare the results from the able-bodied and SCI subject groups, we used a repeated measures analysis of variance (ANOVA) [38]. With the use of the same standard set of joint angles and velocities, calculated moment data were obtained from each subject's moment model. A repeated measures ANOVA was then performed. A *p*-value of less than 0.01 was set to indicate significance. With this statistical test, differences because of subject group, joint velocity, or adjacent joint angle could be determined.

RESULTS

Variability and Sensitivity

The model parameters were fitted to the mean passive moment values for each subject group. The estimated model parameters for the able-bodied and SCI groups are given in **Table 7** and **Table 8,** respectively. We calculated the standard deviations (SDs) of these mean curves to determine the variability of the moment values across each subject group. The ankle joint, where the passive moments

Table 7.
Passive moment model parameters for each joint tested (able-bodied subjects).

Model Parameter	Ankle Inv/Ev	Ankle Flex/Ext	Knee Flex/Ext	Hip Flex/Ext	Hip Ab/Ad
a_1	0.65	2.8	6.1	13.0	16.0
a_2	–2.8	–3.9	–2.3	–0.87	–4.5
a_3	–0.89	–0.49	1.1	0.45	NA
a_4	NA	0.22	–0.82	0.051	–0.27
a_5	–0.63	–0.20	–2.0	–6.3	–4.8
a_6	3.0	4.1	0.50	1.3	2.3
a_7	–0.019	–0.14	–0.15	–0.11	NA
a_8	NA	1.5	–0.47	–0.65	–0.021
k	0.20	0.31	0.20	0.39	1.4
b	0.010	0.10	0.71	4.6	2.2
n	0.083	0.099	0.089	0.20	0.12

Inv/Ev = inversion/eversion Ab/Ad = abduction/adduction
Flex/Ext = flexion/extension NA = not applicable

Table 8.
Passive moment model parameters for each joint tested (subjects with SCI).

Model Parameter	Ankle Inv/Ev	Ankle Flex/Ext	Knee Flex/Ext	Hip Flex/Ext	Hip Ab/Ad
a_1	0.25	3.8	4.3	22.0	17.0
a_2	–4.2	–4.8	–3.6	–1.4	–5.2
a_3	1.1	–1.6	0.33	0.35	NA
a_4	NA	0.22	–0.73	0.16	–0.14
a_5	–0.78	–0.0001	–0.52	–0.83	–4.0
a_6	4.2	15.0	1.3	2.9	3.1
a_7	0.95	1.7	–0.41	–0.66	NA
a_8	NA	–2.7	–0.44	–1.3	–1.1
k	0.33	0.35	0.13	0.53	0.56
b	0.28	0.20	0.27	0.38	0.90
n	0.025	0.037	0.043	0.48	0.14

Inv/Ev = inversion/eversion   Ab/Ad = abduction/adduction
Flex/Ext = flexion/extension   NA = not applicable

were low, exhibited the lowest variability. The SDs for the able-bodied group were on the order of 0.75 Nm, while the values for the SCI group were typically around 0.84 Nm. The hip joint in abduction/adduction exhibited the largest variability. SDs for the able-bodied group were typically 8.95 Nm, while values for the SCI group were on the order of 7.0 Nm.

The mean square error (MSE) between the model data and the experimental data for all the subjects ranged from 0.020 to 5.1 Nm^2. On average, the model predictions for the ankle and knee joints were within ±1 Nm of the experimental data 91 percent (σ = 8.7%) of the time. For hip flexion/extension, the model data were within ±2 Nm of the experimental data 76 percent (σ = 17%) of the time. For hip abduction/adduction, 94 percent (σ = 8.4%) of the fitted data fell within ±2 Nm of the experimental data. As a percentage of the peak-to-peak range for the passive moments, ±2 Nm represents an error of less than ±5 percent.

Although every parameter was necessary for the model, some factors influenced the output more than others. The most influential variable on the sigmoidal shape of the curve was θ; therefore, parameters a_2 and a_6 were the most important. Depending on the joint, the next influential variable would be either the proximal or distal joint angle. The least sensitive variable was then the remaining adjacent joint angle. The model output was eight times (range = 0.7 to 50.0) more sensitive to parameters a_2 and a_6 than to the adjacent joint parameters. The variable that most influenced the amount of hysteresis was joint velocity. Therefore, the hysteresis was most sensitive to parameter *b*.

Passive Moment Magnitudes and Velocity Dependence

While the overall sigmoidal shapes of the passive moment curves were very similar, the magnitudes of the curves differed between subject groups. Using repeated measures ANOVA, we made statistical comparisons between the able-bodied and SCI subjects tested. Using a *p*-value of less than 0.01 to indicate statistical significance, we found the passive moment curves for each subject group to be different at every joint tested except the knee. Subject groups differed significantly at every joint with respect to the influence of the proximal joint angle, while the effect of the distal joint angle was significant only for hip abduction/adduction.

The effect of joint velocity on passive moments was similar at every joint for both groups. Except for the hip (abduction/adduction) and the ankle (plantar flexion/dorsiflexion) joints of the SCI group, joint velocity had a statistically significant influence on the passive moment at all joints for both groups. Therefore, the amount of hysteresis exhibited by the passive moment curves was significant for these joints. Consistent with previous reports [13,19,39], the influence of joint velocity on the passive joint moment at magnitudes above 10°/s was quite small for both subject groups.

Individual Joint Moment Measurements

Ankle Joint Plantar Flexion and Dorsiflexion

Figure 4 presents the passive joint moments and SDs at the ankle joint in plantar flexion and dorsiflexion for a typical able-bodied and SCI subject. As the joint rotated away from the neutral position (0 Nm), moments developed in both subjects to resist the movement. The repeated measures ANOVA for each subject group showed that the distal joint angle (ankle inversion/eversion) did not have a statistically significant effect on the passive moment for either subject group (**Figures 4(a) and 4(b)**). Conversely, the ANOVA showed that the proximal joint (i.e., the knee) had a significant (p < 0.01) effect on the ankle moment (**Figures 4(c) and 4(d)**). As the knee joint was extended, the ankle joint became stiffer in the plantar flexion/dorsiflexion direction.

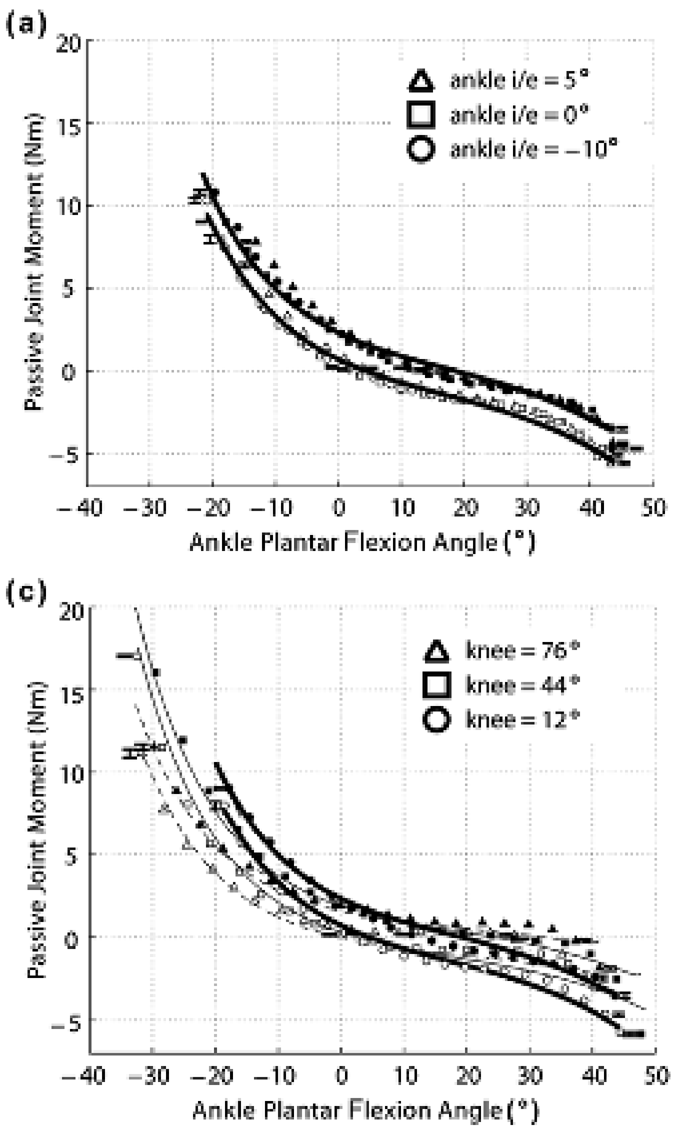

Figure 4.
Passive ankle plantar flexion/dorsiflexion moments at 10°/s for **(a)** and **(c)** an able-bodied subject and **(b)** and **(d)** an SCI subject. **(a)** and **(b)** Effect of ankle eversion angle with knee angle fixed. **(c)** and **(d)** Effect of knee flexion angle with ankle eversion angle fixed. Symbols represent experimental data. Lines represent model data. Filled symbols represent joint movements from large angles to small angles and open symbols represent movements from small angles to large angles. Standard deviations of experimental data are indicated at ends and middle of range of motion. Mean square error (MSE) for able-bodied subject = 0.32. MSE for SCI subject = 0.18 (i/e = inversion/eversion).

Knee Joint Flexion and Extension

As for the ankle, passive resistive moments were generated at the knee whenever it was rotated away from its neutral position. **Figure 5** shows typical knee moments for an able-bodied and an SCI subject. Repeated measures ANOVA indicated that ankle angle (plantar flexion/dorsiflexion) had an insignificant effect on the knee moment for both subject groups. **Figures 5(a)** and **5(b)** illustrate this result for an able-bodied and SCI subject. The influence of the hip angle (flexion/extension) was calculated to be significant in both subject groups, as illustrated in **Figures 5(c)** and **5(d)**. At flexed hip postures, the passive knee moment increased as the knee was extended. As the hip joint moved into extension, the passive moment magnitude increased as the knee was flexed.

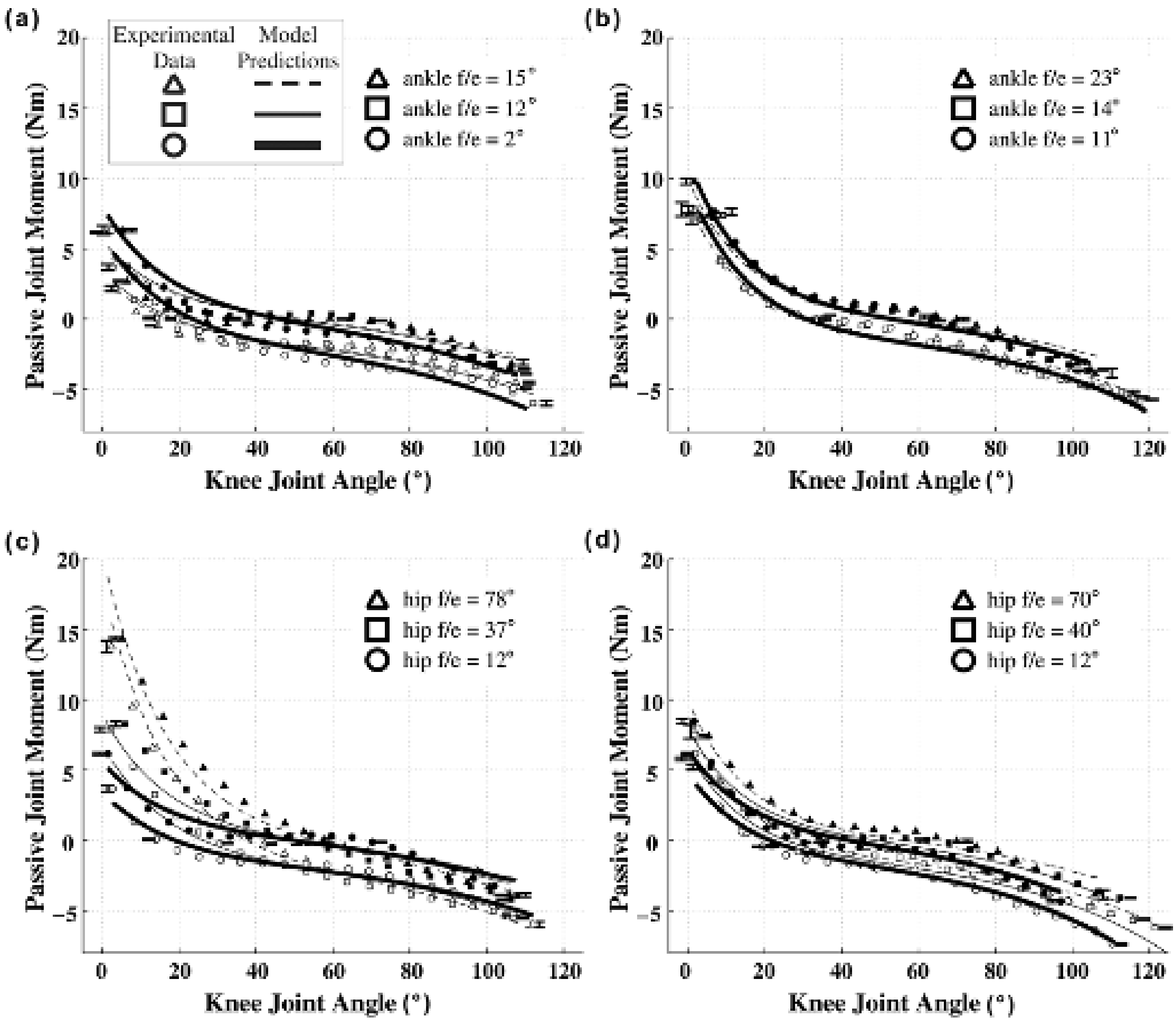

Figure 5.
Passive knee moments at a constant velocity for **(a)** and **(c)** an able-bodied subject and **(b)** and **(d)** an SCI subject. **(a)** and **(b)** Effect of ankle plantar flexion angle at a constant hip angle. **(c)** and **(d)** Effect of hip flexion angle at a constant ankle angle. Mean square error (MSE) for able-bodied subject = 0.35. MSE for SCI subject = 0.25 (f/e = flexion/extension).

Hip Joint Flexion and Extension

Extending the knee increased the magnitude of the hip moments as the hip was flexed for both subject groups (**Figures 6(a)** and **6(b)**). As the knee was flexed, increased hip moments developed in both subject groups as the hip was moved into extension. The passive moments at the hip joint were significantly influenced by the hip abduction/adduction and knee joint angles. Changes in the hip abduction/adduction angle tended to shift the passive moment curve laterally (**Figures 6(c)** and **6(d)**).

Ankle Joint Inversion and Eversion

Example results from rotating the ankle joint in the inversion/eversion direction are displayed in **Figure 7**. As the joint was rotated to the end of its ROM, passive moments developed to restore the joint to its neutral position in both the able-bodied subject and the SCI subject.

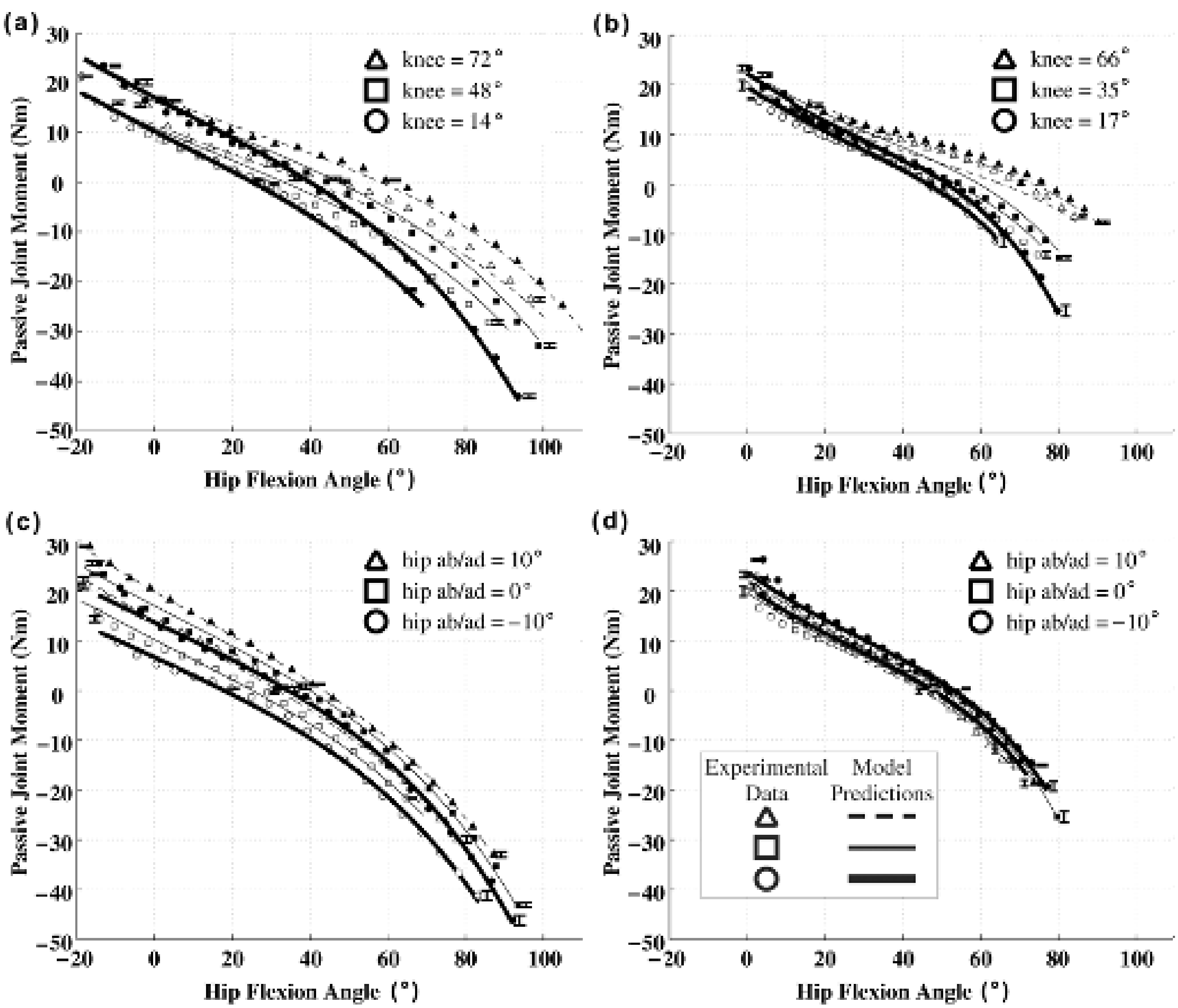

Figure 6.
Passive hip flexion/extension moments at 10°/s for **(a)** and **(c)** an able-bodied subject and **(b)** and **(d)** an SCI subject. **(a)** and **(b)** Effect of knee flexion angle with hip abduction held constant. **(c)** and **(d)** Effect of hip abduction angle with knee angle held constant. Mean square error (MSE) for able-bodied subject = 1.7. MSE for SCI subject = 2.0 (ab/ad = abduction/adduction).

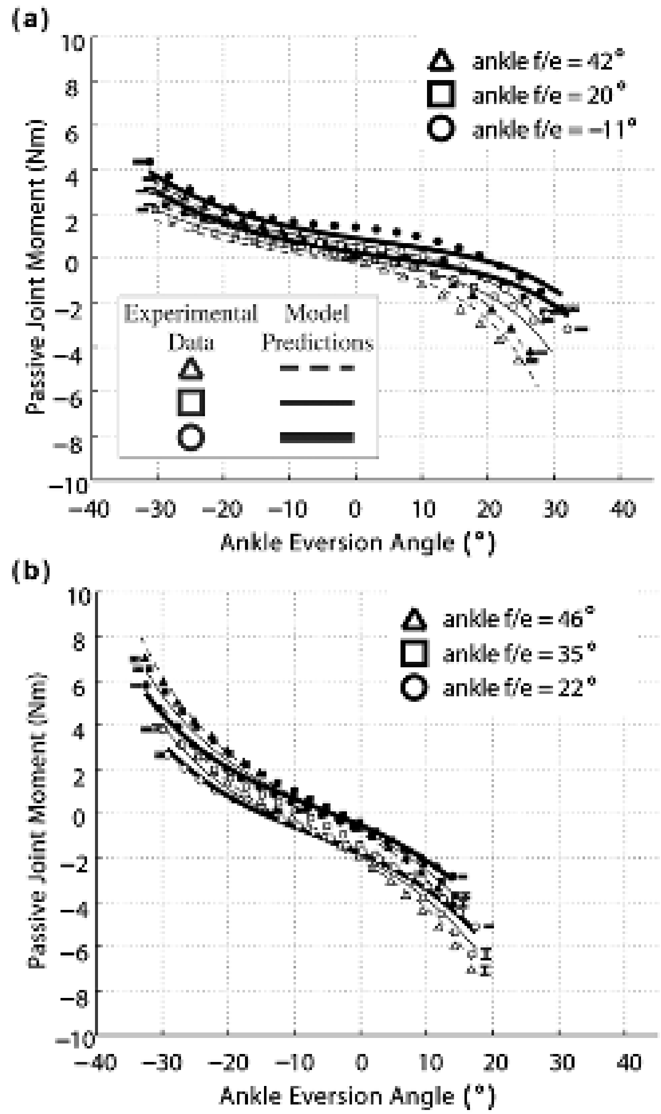

Figure 7.
Passive ankle inversion/eversion moments at a velocity 30°/s for **(a)** an able-bodied subject and **(b)** an SCI subject. Ankle plantar flexion angle was set at three different values. Mean square error (MSE) for able-bodied subject = 0.040. MSE for SCI subject = 0.034 (f/e = flexion/extension).

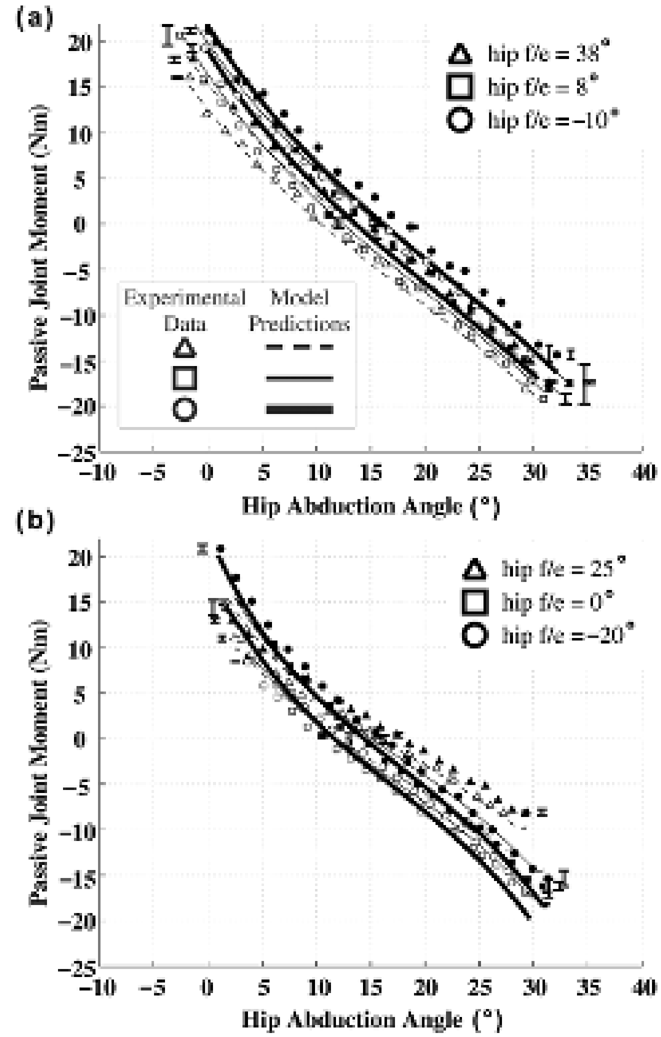

Figure 8.
Passive hip abduction/adduction moments for **(a)** an able-bodied subject and **(b)** an SCI subject. Velocity was fixed at 10°/s. Hip flexion/extension (f/e) angle was set at three different values. Mean square error (MSE) for able-bodied subject = 1.6. MSE for SCI subject = 2.4.

The plantar flexion/dorsiflexion angle had no statistically significant effect for the SCI subject group, but the proximal joint did have a significant effect for the able-bodied group.

Hip Joint Abduction and Adduction

Illustrated in **Figure 8** are the passive moments measured during hip abduction/adduction from an able-bodied subject and SCI subject. The passive moment magnitudes increased as the joint reached its end ROM. The influence of the hip flexion/extension angle on the abduction/adduction moment was statistically significant for both subject groups.

DISCUSSION

In this study, we measured the passive moments of five joint actions of the human lower limb (flexion/extension of the ankle, knee, and hip; ankle inversion/eversion; and hip abduction/adduction) in both able-bodied individuals and in individuals with paralysis arising from SCI. For all subjects and joints, imposed movements away from the neutral position of the joint generated resistance that increased as the joint approached the end of its ROM. The adjacent joint angles were also determined to have statistically significant influences on the passive moments of the primary joint. The data from both able-bodied subjects and SCI subjects were very similar in shape. The shape and magnitudes of the observed passive moments measured for the ankle, knee, and hip joints in flexion and extension were consistent with those of previously reported studies [15,16,18,19]. Any differences between the moment values observed and the values reported in the literature may be a result of natural intersubject variability.

Experimental Limitations

The experiments of this study consisted of passively rotating a joint while measuring the resistance to movement. To remove the inertial effects of the limb, joints were rotated at a constant velocity. However in practice, the dynamometer needed to accelerate and decelerate as the joint changed direction from flexion to extension. Consequently, these accelerations caused inertial effects near the end of the joint's ROM. As a result, for trials with high velocities and high limb weights, the inertial effects were the greatest. To remove these effects, we used only the range of data points when the joint velocity was constant in the data analysis. However, remnant inertial effects are a possible reason the hip flexion/extension trials, which had the largest limb weights, exhibited the poorest fit between the model and experimental data.

The moment caused by the weight of the limbs was estimated with regression equations and, therefore, was also a potential source of error. Passive moment measurements about a vertical axis would have minimized the effects of limb weight. However, the experimental apparatus did not allow for measurements about a vertical axis. Therefore, regression equations were employed, because they provided a consistent method for the limb weight calculation.

Model Performance

We used a nonlinear viscoelastic model in this study to provide a single tool that could describe the most important characteristics of the passive joint moments throughout the ROM to determine similarities and differences between the study populations. The passive moment model captured the nonlinear elastic properties at the joint, which determined the overall shape of the curve, and the nonlinear viscous properties, which affected the amount of hysteresis exhibited by the curve. The model did not capture the properties of an unconditioned joint, so this model was not suitable for examining the effect of conditioning.

The calculated MSE values indicated a good fit between the model and the experimental data [16]. The high percentage of model data within ±1 Nm of the experimental data also indicated that the model predictions were close to the experimental data. Under these conditions, the model would be sufficient for predicting the passive joint moments that would develop. Furthermore, it was able to identify several commonalities and differences between the two sample groups. This finding suggests that the model may prove to be a useful tool for exploring and understanding the effects of passive joint moments in other studies of human movement.

Influence of Proximal and Distal Joints

For ankle dorsiflexion, the knee angle had an influence on the ankle moment because of the biarticular gastrocnemius muscle, which crosses both the knee and the ankle joints. However, at the knee joint, the ankle plantar flexion/dorsiflexion had little influence on the knee passive moment. The hip and the knee joints are coupled through the hamstring and the rectus femoris muscles. The hip flexion/extension angle did affect the knee moments of the able-bodied subjects in both knee flexion and extension. However, for the SCI subjects, hip angle only affected knee moments between neutral and fully flexed. This finding suggests that the rectus femoris coupling is present in both groups, but the SCI subjects had a diminished hamstring effect. Coupling between the knee and hip also resulted in the knee angle having an influence on the hip flexion/extension passive moment in both subject populations. Hip abduction/adduction was expected to have an influence on the hip flexion/extension moment, because it would be affecting the same tissues as hip flexion/extension. This finding was found to be true for both subject groups. Similarly, hip flexion/extension was found to influence the hip abduction/adduction passive moment. Ankle flexion/extension was expected to affect the ankle inversion/eversion moment because several muscles cross both joints—the able-bodied group had a significant difference, but the SCI group had no difference.

Comparisons Between Subject Groups

For every joint except the knee, the SCI group had a majority of passive moment magnitudes that were larger than the able-bodied group. This implies that the SCI group had stiffer joints compared to the able-bodied group. Possible mechanisms for the differences observed between subject groups are changes in the moment arms at the joint, changes in the fascia that hold these tissues in place, or transformations of the musculotendon units following SCI [3].

Important to note is that these experiments were only performed on a sample size of four individuals with SCI and five able-bodied individuals. Neither group can be considered to represent their entire population. The able-bodied volunteers were a convenience sample of healthy young graduate students in our laboratory. The subjects with SCI were experienced users of FES standing systems and, therefore, were required to have healthy and stable enough joints for weight-bearing and near-normal ROMs before being recruited into this study [40]. Therefore, one should be cautioned against generalizing these results to the whole SCI and able-bodied populations or to other populations who were not examined, such as persons with joint disease. Also, the large variability between subjects may limit the capability to use the group averages to represent any single individual. However, the group averages were useful for examining the capability of the model to fit to the experimental data. In addition, these preliminary data have provided a framework for further investigation as more subjects are tested, which would include understanding the magnitudes and causes of variability between the passive moment values of individual subjects.

CONCLUSIONS

In this study, the passive moments generated about ankle inversion/eversion; hip abduction/adduction; and ankle, knee, and hip flexion/extension were characterized for able-bodied volunteers and individuals with SCIs. The passive moment curves from the two subject groups displayed similar shapes but significant differences in passive moment values. The passive moment values were significantly different at every joint except the knee. The differences indicate that the SCI group had stiffer joints. From this limited sample, this suggests able-bodied passive properties cannot be assumed to be the same as SCI passive properties.

The influence of adjacent joints on the passive moments was also examined. The majority of the results indicated that the positions of adjacent joints significantly influenced the passive moment about a joint. The only adjacent joint angles that were not significantly influential were the ankle plantar flexion/dorsiflexion angle on the knee passive moment for both subject groups and ankle plantar flexion/dorsiflexion on the ankle inversion/eversion moment for the SCI group. Therefore when measuring or estimating passive joint moments, one should include the effects of adjacent joint angles.

A mathematical equation was developed to describe the passive lower-limb joint moments, was successfully fitted to experimental data at each joint, and was used to compare the passive moment values of the two subject groups. With this generalized model, one equation was able to describe both the elastic and viscous properties of a joint. One advantage of this model is its compact form, which employs a relatively small number of physiologically relevant parameters that capture the salient features of the passive moment curves at each joint and allows for a single equation to describe the passive moments throughout the ROM. Furthermore, this new tool can also be customized to a particular segment of the ROM, for example, the narrow segment of the joint ROMs exhibited during quiet upright standing. For these specialized cases, the nonlinear viscoelastic model developed in this study can be adjusted to provide improved accuracy for the particular study being undertaken. In addition, parameters of the model can be easily changed to reflect contractures, disease states, or other joint conditions.

Future work can use this model as part of a larger musculoskeletal model of the lower limbs for computer simulation studies of bipedal function. For example, one can use a musculoskeletal model that incorporates a realistic representation of the passive moment generating capacities of the hip, knee, and ankle to perform computer simulation studies to investigate how passive moment properties such as contractures can affect functional movements. One can also examine interventions to alter passive joint properties (e.g., tendon lengthening) in simulation to gain insight into their effect on standing and walking function. We also intend to use such a strategy to examine whether passive properties can be varied to increase one's functional ability after an SCI and to predict their effect on the performance of controllers for advanced FES systems for standing and walking.

ACKNOWLEDGMENTS

We wish to thank the subjects that participated in this study and Mr. Jim Uhlir, Mr. Mark Pierre, Ms. Lucy Kim, and Dr. Musa Audu for their assistance with the experimental testing.

REFERENCES

1. Fung YC. Biomechanics: Mechanical properties of living tissues. 2nd ed. New York: Springer-Verlag; 1993. p. 254–62, 525–35.
2. Patrick JH, Farmer SE, Bromwich W. Muscle stretching for treatment and prevention of contracture in people with spinal cord injury. Spinal Cord 2002;40(8):421–22.
3. Burnham R, Martin T, Stein R, Bell G, MacLean I, Steadward R. Skeletal muscle fibre type transformation following spinal cord injury. Spinal Cord 1997;35(2):86–91.
4. Castro MJ, Apple DF Jr., Hillegass EA, Dudley GA. Influence of complete spinal cord injury on skeletal muscle cross-sectional area within the first 6 months of injury. Eur J Appl Physiol Occup Physiol 1999;80(4):373–78.
5. Covault J, Merlie JP, Goridis C, Sanes JR. Molecular forms of N-CAM and its RNA in developing and denervated skeletal muscle. J Cell Biol 1986;102(3):731–39.
6. Kagaya H, Sharma M, Kobetic R, Marsolais EB. Ankle, knee, and hip moments during standing with and without joint contractures: simulation study for functional electrical stimulation. Am J Phys Med Rehabil 1998;77(1):49–54.
7. Gottlieb GL, Agarwal GC. Dependence of human ankle compliance on joint angle. J Biomech 1978;11(4):177–81.
8. Agarwal GC, Gottlieb GL. Compliance of the human ankle joint. Trans Am Soc Mech Eng 1977;99(3):166–70.
9. Goddard R, Dowson D, Longfield MD, Wright V. The measurement of stiffness in human joints. Rheologica Acta 1969;Band 8(Heft 2):229–34.
10. Such CH, Unsworth A, Wright V, Dowson D. Quantitative study of stiffness in the knee joint. Ann Rheum Dis 1975; 34(4):286–91.
11. Wright V, Johns RJ. Quantitative and qualitative analysis of joint stiffness in normal subjects and in patients with connective tissue diseases. Ann Rheum Dis 1961;20:36–46.
12. Duong B, Low M, Moseley AM, Lee RY, Herbert RD. Time course of stress relaxation and recovery in human ankles. Clin Biomech (Bristol, Avon) 2001;16(7):601–7.
13. Esteki A, Mansour JM. An experimentally based nonlinear viscoelastic model of joint passive moment. J Biomech 1996;29(4):443–50.
14. Hayes KC, Hatze H. Passive visco-elastic properties of the structures spanning the human elbow joint. Eur J Appl Physiol 1977;37(4):265–74.
15. Yoon YS, Mansour JM. The passive elastic moment at the hip. J Biomech 1982;15(12):905–10.
16. Edrich T, Riener R, Quintern J. Analysis of passive elastic joint moments in paraplegics. IEEE Trans Biomed Eng 2000;47(8):1058–65.
17. Knutson JS, Kilgore KL, Mansour JM, Crago PE. Intrinsic and extrinsic contributions to the passive moment at the metacarpophalangeal joint. J Biomech 2000;33(12):1675–81.
18. Mansour JM, Audu ML. The passive elastic moment at the knee and its influence on human gait. J Biomech 1986;19(5): 369–73.
19. Riener R, Edrich T. Identification of passive elastic joint moments in the lower extremities. J Biomech 1999;32(5): 539–44.
20. McFaull SR, Lamontagne M. The angular damping coefficient of the in vivo human knee joint. In: XIV ISB Congress. Paris, France; 1993.
21. McFaull SR, Lamontagne M. The passive elastic moment about the in vivo human knee joint. In: XIV ISB Congress. Paris, France; 1993.
22. Hatze H. A new method for the simultaneous measurement of the movement of inertia, the damping coefficient and the location of the centre of mass of a body segment in situ. Eur J Appl Physiol Occup Physiol 1975;34(4):217–26.
23. Vrahas MS, Brand RA, Brown TD, Andrews JG. Contribution of passive tissues to the intersegmental moments at the hip. J Biomech 1990;23(4):357–62.
24. Hatze H. A three-dimensional multivariate model of passive human torques and articular boundaries. Clin Biomech 1997;12(2):128–35.
25. Piziali RL, Rastegar JC. Measurement of the nonlinear, coupled stiffness characteristics of the human knee. J Biomech 1977;10(1):45–51.
26. Lakes RS, Vanderby R. Interrelation of creep and relaxation: a modeling approach for ligaments. J Biomech Eng 1999; 121(6):612–15.
27. Knutson JS. Characterizing the passive moment at the second metacarpophalangeal joint of neuroprosthesis users and able-bodied individuals [master's degree]. Cleveland (OH): Case Western Reserve University; 1997.
28. Davoodi R, Andrews BJ. Computer simulation of FES standing up in paraplegia: a self-adaptive fuzzy controller with reinforcement learning. IEEE Trans Rehabil Eng 1998; 6(2):151–61.

29. Kralj A, Jaeger RJ, Munih M. Analysis of standing up and sitting down in humans: definitions and normative data presentation. J Biomech 1990;23(11):1123–38.
30. Kotake T, Dohi N, Kajiwara T, Sumi N, Koyama Y, Miura T. An analysis of sit-to-stand movements. Arch Phys Med Rehabil 1993;74(10):1095–99.
31. Riley PO, Schenkman ML, Mann RW, Hodge WA. Mechanics of a constrained chair-rise. J Biomech 1991; 24(1):77–85.
32. Doorenbosch CA, Harlaar J, Roebroeck ME, Lankhorst GJ. Two strategies of transferring from sit-to-stand; the activation of monoarticular and biarticular muscles. J Biomech 1994;27(11):1299–307.
33. Lebiedowska MK, Fisk JR. Passive dynamics of the knee joint in healthy children and children affected by spastic paresis. Clin Biomech (Bristol, Avon) 1999;14(9):653–60.
34. Woo SL. Mechanical properties of tendons and ligaments. I. Quasi-static and nonlinear viscoelastic properties. Biorheology 1982;19(3):385–96.
35. Zatsiorsky V, Seluyanov V. Biomechanics VIII-B. In: Matsui H, Kobayashi K, editors. The mass and inertia characteristics of the main segments of the human body. Champaign (IL): Human Kinetics; 1983. p. 1152–59.
36. de Leva P. Adjustments to Zatsiorsky-Seluyanov's segment inertia parameters. J Biomech 1996;29(9):1223–30.
37. Mendenhall W, Sincich T. Statistics for engineering and the sciences. 3d ed. San Francisco (CA): Dellen Publishing Company; 1992. p. 963.
38. S-Plus 2000 Guide to statistics, Volume 1. Seattle (WA): Data Analysis Products Division, Mathsoft; 1999. p. 584–87
39. Roberson L, Giurintano DJ. Objective measures of joint stiffness. J Hand Ther 1995;8(2):163–66.
40. Davis JA, Triolo RJ, Uhlir J, Bieri C, Rhode L, Lissy D, Kukke S. Preliminary performance of a surgically implanted neuroprosthesis for standing and transfers—Where do we stand? J Rehabil Res Dev 2001;38(6):609–17.

Submitted for publication January 6, 2003. Accepted in revised form July 31, 2003.